

Periodic microwave absorption in superconductors

J. Martinek and J. Stankowski

Institute of Molecular Physics, Polish Academy of Sciences, Smoluchowskiego 17, 60-179 Poznań, Poland

(Received 25 March 1994)

A model explaining the presence of a periodic train of microwave absorption lines in the magnetic modulated microwave absorption (MMMA) spectra of high- and low-temperature superconductors is proposed. The model assumes the occurrence of regular superconducting current loops, closed by Josephson junctions, in these materials. The system of such loops is considered within the basic model of the rf superconducting quantum interference device taking into account the effect of thermal fluctuations. The magnetic-field and temperature dependencies of the MMMA obtained on the basis of the proposed model are in qualitative agreement with experimental data.

INTRODUCTION

Measurements of magnetically modulated microwave absorption (MMMA) have proved to be a very sensitive method of determining the critical temperature of the conductor-superconductor phase transition and, have been commonly used for detection of the superconducting state. For granular and irregularly defected superconducting samples the shape of an MMMA signal is similar to that of the derivative of a Lorentz-type line whose typical representative is an electron-paramagnetic-resonance (EPR) line obtained using the modulation technique, but has the reversed phase.¹⁻⁴ This line is observed in zero magnetic field, where microwave absorption has a sharp minimum. In higher magnetic field microwave absorption slowly and linearly increases with magnetic field. Against a background of a broad signal we observe the noiselike fluctuations or oscillations which are reproducible and periodical. Such trains of peaks, periodic in the field scale, have been observed for samples of twinned monocrystals of cuprate superconductors of regular form⁵⁻⁹ as well as for low-temperature superconductors; the best signal has been observed for two small irregular pieces touching each other.¹⁰⁻¹² The observed trains of peaks made a series of well-resolved lines that were periodic in the externally applied magnetic field. The spacing of the lines in the spectra is determined by a macroscopic flux quantization, which leads to a conclusion about the presence of superconducting current loops in these materials. To explain the observed spectrum Xia and Stroud¹³ have proposed a simple model in which the basic idea is to consider junctions connected into a loop and to look for the ground-state energy of this system. Later Vichery, Benney, and Lejay⁷ developed this model on the basis of the work of Silver and Zimmerman¹⁴ explaining the origin of the microwave power threshold in the MMMA signal.

In this paper, we propose a precise model of MMMA which, apart from basic properties of the signal such as periodicity and power threshold, can explain the shape of individual lines in the MMMA signal, and changes in the spectrum shape induced by varying temperature or intensity of an external dc magnetic field. The proposed model

can also account for the results of the microwave scan experiment,⁸ i.e., the MMMA signal as a function of the microwave-field power at nominally zero dc field. The model assumes the formation of regular superconducting current loops closed by Josephson junctions in the studied materials. Under this assumption we investigate the origin of microwave absorption adapting the basic model of the rf superconducting quantum interference device¹⁵ (SQUID) taking into account the thermal fluctuations.¹⁶⁻¹⁸ We present the results of detailed calculations of the MMMA spectra and their characteristic dependencies on magnetic field, microwave power, and temperature which well describe the earlier reported experimental data.⁵⁻¹²

MODEL OF THE rf SQUID

A magnetic flux threading a superconducting ring of the area S , closed by a single Josephson junction¹⁵ is given by the expression

$$\varphi + \beta \sin \varphi = \varphi_x, \quad (1)$$

where $\beta \equiv 2\pi L I_c / \Phi_0$ is the dimensionless inductance, φ_x is the external magnetic-field flux in the units of $\Phi_0/2\pi$, and φ is the magnetic flux threading the loop in the units of $\Phi_0/2\pi$. I_c is the critical current of the junction and L is the loop inductance. There are essentially two different modes in which such a system (rf SQUID) can operate, depending on the $\varphi(\varphi_x)$ dependence. If $\beta \leq 1$, then $\varphi(\varphi_x)$ increases monotonically and the rf SQUID is in the dispersive mode. If $\beta > 1$, the $\varphi(\varphi_x)$ dependence is multivalued, and hysteretic. When the amplitude of the rf applied flux is greater than a critical value, the hysteresis loops are spanned, and energy is dissipated by the system. This mode is called dissipative. In the stationary state, the total energy of the rf SQUID is composed of the energy of the Josephson junction and the magnetic energy stored in the loop:¹⁵

$$U = \epsilon_c [1 - \cos \varphi + (\varphi - \varphi_x)^2 / 2\beta], \quad (2)$$

where $\epsilon_c = \Phi_0 I_c / 2\pi$. In the case when $\beta \leq 1$, the $U(\varphi)$ dependence has one minimum corresponding to the

unambiguous stable solution of Eq. (1). For $\beta > 1$ the $U(\varphi)$ function may have a few local minima and maxima. Change of the external flux φ_x will induce jumps of the system between local minima. From (2) we can find the values of φ and φ_x at which the system makes a transition between two subsequent minima:

$$\begin{aligned}\varphi^k &= 2\pi n \pm \arccos[\beta^{-1}], \\ \varphi_x^k &= 2\pi(n+1) \pm \varphi_{th},\end{aligned}\quad (3)$$

where

$$\varphi_{th} = (\beta^2 - 1)^{1/2} + \arccos(-\beta^{-1}),$$

for $n = 0, \pm 1, \pm 2, \dots$

The energy difference between the two subsequent stable states, ϵ , [Fig. 1(b)] corresponds to the energy the system loses upon the transition. The relationship between the value of this energy, ϵ , and β , the parameter characterizing a studied system, may be found numerically¹⁶ from Eqs. (1) and (2) to be approximately

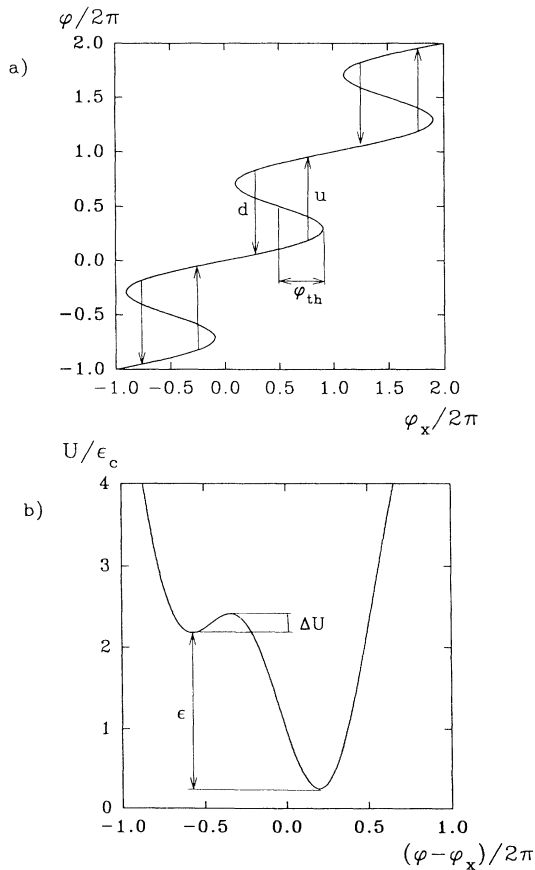


FIG. 1. (a) Internal flux φ versus applied flux φ_x for a superconducting loop with a Josephson junction. Arrows indicate thermally activated transition to a state of the higher (u) and the lower (d) value of the internal flux. (b) Free-energy function for $\varphi_x = 2/3\pi$ versus $\varphi - \varphi_x$, where ΔU is an energy barrier and ϵ is the energy difference between the two metastable states of the transition. Both curves refer to the case $\beta = 2\pi L I_c / \Phi_0 = 4$.

$$\epsilon = \begin{cases} 0, & \beta \rightarrow 1 \\ \Phi_0 I_c - \Phi_0^2 / 2L, & \beta \gg 1. \end{cases}\quad (4)$$

For temperatures higher than the absolute zero, the stationary states become metastable as a consequence of thermal fluctuations. The lifetime associated with the flux remaining in a given state is then¹⁶⁻¹⁸

$$\tau = \left[\frac{\omega_c (2\Delta\varphi_x)^{1/2} (\beta^2 - 1)^{1/4}}{\beta} \right]^{-1} \exp(\Delta U / k_B T), \quad (5)$$

where $\omega_c = R/L$ is the characteristic frequency of the loop related to its relaxation time and R is the weak link normal resistance. For typical superconductors this frequency is of an order of 10^{12} Hz.¹⁶ ΔU is the energy barrier against a flux transition between two subsequent minima [Fig. 1(b)] which can be found from (2)

$$\Delta U = \epsilon_c 2 \left[\frac{8}{9} \right]^{1/2} \frac{(\Delta\varphi_x)^{3/2}}{\beta(\beta^2 - 1)^{1/4}}, \quad (6)$$

where $\Delta\varphi_x \equiv |\varphi_x^k - \varphi_x|$. The above formulas (5) and (6) are valid in the case of small thermal fluctuations:

$$k_B T \ll \Delta U. \quad (7)$$

Because of thermal fluctuations, a transition to a neighboring state takes place much earlier than at the time when the resultant flux reaches the critical value φ_x^k . Distribution of applied flux at which the jump occurs depends on how φ_x evolves in time. The probability that a decay has taken place is given by

$$q(t) = 1 - \exp \left[- \int_{-\infty}^t \frac{ds}{\tau[\Delta\varphi_x(s)]} \right]. \quad (8)$$

Let us consider the situation when a tank circuit of inductance L_T and capacitance C_T , rf excited at the resonance frequency ω , is loosely coupled by a mutual inductance M to the SQUID. Let us assume that then a superconducting loop is exposed to a dc external magnetic field H_0 perpendicular to the plane of the loop and an ac magnetic field $H_1 \sin(\omega t)$ from the tank circuit parallel to H_0 . In such a case the magnetic flux passing through the loop can be described by the equation

$$\varphi_x(t) = \hat{\varphi}_x + a \cos(\omega t), \quad (9)$$

where $\hat{\varphi}_x = 2\pi S H_0 / \Phi_0$ is the constant external flux, $a = 2\pi S H_1 / \Phi_0$ the amplitude of the variable flux. When this amplitude reaches the value¹⁶

$$a_1(\hat{\varphi}_x) \equiv \varphi_{th} + \pi - |\hat{\varphi}_x - 2\pi n|, \quad |\hat{\varphi}_x - 2\pi n| \leq \pi \quad (10)$$

two quantum transitions take place within each period in the SQUID and at each of them the system loses the energy 2ϵ . As a result of the energy loss by the tank circuit, the amplitude of the flux oscillations gets rapidly decreased by

$$\delta a = 2\pi k^2 / a\beta \ll a_1, \quad (11)$$

so in the next cycle the condition (10), where $k^2 = M^2 / LL_T$ is the coefficient of the coupling of the su-

perconducting loop and the rf tank circuit, may not be satisfied. Between transitions, the level of the amplitude builds back up. Whether the subsequent jump takes place or not depends on the value of the amplitude before the last jump, i.e., on the course of previous cycles. This process may have a very long period or may be aperiodic (chaotic).¹⁸ When the amplitude reaches the value

$$a_2(\hat{\varphi}_x) \equiv \varphi_{th} + \pi + |\hat{\varphi}_x - 2\pi n|, \quad |\hat{\varphi}_x - 2\pi n| \leq \pi \quad (12)$$

then within the same period of the flux another pair of jumps can take place. When further increasing amplitude reaches the value a_3 , a third pair of transitions appears. The critical values of the amplitude at which the system begins traversing subsequent hysteresis loops during a single cycle satisfy the condition

$$a_{k+2} = a_k + 2\pi. \quad (13)$$

Considering the effect of thermal fluctuations on the behavior of such a system, we can find the probability of a jump between two neighboring energy minima induced by thermal fluctuations. In order to do that, we shall rewrite the expression for the flux (9) in the form

$$\Delta\varphi_x \cong \bar{a} - a(\omega t)^2/2, \quad \bar{a} \equiv a_k - a \quad (14)$$

and from (8) we get¹⁶

$$q = 1 - \exp \left\{ -C \int_u^\infty \frac{z^{1/2} dz}{(z-u)^{1/2}} \exp(-z^{3/2}) \right\}, \quad (15)$$

$$C = \frac{(\beta^2 - 1)^{1/4}}{2\pi\beta a^{1/2}} \left[\frac{\omega_c}{\omega} \right] \Delta a,$$

where u is the normalized value of \bar{a}

$$u = \bar{a}/\Delta a, \quad \Delta a \equiv \left[\frac{\beta(\beta^2 - 1)^{1/4} \gamma}{2(8/9)^{1/2}} \right]^{2/3} \cong \beta \left[\frac{\gamma}{2} \right]^{2/3} \quad (16)$$

and $\gamma = k_B T / \varepsilon_c$ is the normalized temperature. For $u \geq 1$ from (15) we have

$$q(u) = 1 - \exp[-Yu^{1/4} \exp(-u^{3/2})], \quad (17)$$

$$Y = \left[\frac{2}{3\pi} \right]^{1/2} \left[\frac{\omega_c}{\omega} \right] \left[\frac{\gamma}{2} \right]^{2/3} \gg 1,$$

whereas for $u \ll 1$ we assume $q = 1$. The change in the $q(u)$ function from zero to one takes place within an interval of Δa in length for

$$u = u_0 \cong \ln^{2/3}[Y \ln^{1/6}(Y)]. \quad (18)$$

If the following condition is fulfilled:

$$\frac{2\pi k^2}{\beta^3} \ll \left[\frac{\gamma}{2} \right]^{2/3}, \quad (19)$$

then Δa is much greater than the scatter δa of the amplitude due to the absorption of power upon jumps of the phase. In such circumstances, the system behavior does not depend on the history of the process, which can be correctly described taking into account only the influence

of fluctuations while q determines exactly the probability of the studied phenomenon.

MAGNETICALLY MODULATED MICROWAVE ABSORPTION

The loss of energy (absorption of power) in the rf SQUID as a function of an external flux may be described by the following equation:

$$P(\hat{\varphi}_x) = E \frac{\omega}{2\pi} \sum_{n=-\infty}^{\infty} q_{u,n} q_{d,n}, \quad (20)$$

where

$$q_{u,n} = q \left[\frac{\varphi_{th} - a + [2\pi(n+0.5) + \hat{\varphi}_x]}{\Delta a} \right]$$

and

$$q_{d,n} = q \left[\frac{\varphi_{th} - a - [2\pi(n+0.5) + \hat{\varphi}_x]}{\Delta a} \right]$$

are the probabilities of jumping of the flux threading the ring to a higher (u —up) or a lower (d —down) value [Fig. 1(a)]. The product $q_{u,n} q_{d,n}$ is the probability of the system completing one full hysteresis loop. The symbol E stands for the energy absorbed when the hysteresis is spanned once, i.e., it is the area of the hysteresis loop in the i -vs- φ_x space. In the absence of fluctuation, the quantity E is well approximated by 2ε from Eq. (4). Thermal fluctuations causing the jump to occur long before the external flux φ_x reaches the critical value φ_x^k are also responsible for diminishing the effective area of the hysteresis loop. In view of the above, the lost energy E can be expressed, using (18), as

$$E \cong \begin{cases} 2\varepsilon(1 - u_0 \Delta a / \varphi_{th}), & \varphi_{th} > u_0 \Delta a \\ 0, & \varphi_{th} \leq u_0 \Delta a. \end{cases} \quad (21)$$

The MMMA technique in the standard EPR spectrometer provides a modulated signal at the modulation frequency (100 kHz) for phase-sensitive detection which yields a signal proportional to the derivative of the microwave absorption for a small modulation field.⁸ Thus, an MMMA signal is described by the derivative of Eq. (20) which takes the form

$$\frac{dP}{d\hat{\varphi}_x} = E \frac{\omega}{2\pi} \sum_{n=-\infty}^{\infty} (q'_{u,n} q_{d,n} + q_{u,n} q'_{d,n}), \quad (22)$$

where prime denotes the derivative of the probability function with respect to $\hat{\varphi}_x$ and n numbers subsequent hysteresis loops in φ -vs- φ_x space [Fig. 1(a)].

According to (22) a single symmetric MMMA line is composed of two parts, known as the upper and the lower lobes, corresponding to the first and the second components of the expression following the sum sign in (22). The first one corresponds to the positive while the second to the negative values of an MMMA signal. For high values of the microwave field, these lobes become separated enough so that the shape of each of them can be seen. The shape of the lobe which corresponds to the derivative

of the probability q [Eq. (15)] (Refs. 16 and 17) is similar to the shape of the experimental spectrum obtained by Muromtsev *et al.*,¹⁹ with high resolution of the magnetic field so that the shape of individual line has been well marked. Although a single MMMA line is symmetric, one of its lobes after separation becomes clearly asymmetric; one of lobe corners is sharp whereas the other is wide like the curve in Refs. 16 and 17.

MMMA spectra as a function of external dc magnetic field H_0 for various microwave power levels can be calculated from (22). For a given value H_0 the summation in (22) may include only the components due to these hysteresis loops which are swept by the microwave variable magnetic field H_1 , as the other components are zero. In our calculations we have assumed that the microwave-field frequency in the X band is 9.4 GHz. The internal parameters of the system (I_c, S, β) were adjusted so that the results would be similar to those obtained by Kish, Tyagi, and Kraft.⁸ Figure 2 shows the simulation of MMMA spectra for $I_c = 3 \times 10^{-5}$ A, $\beta = 2.6$, $T = 10$ K, and $S = 100 \mu\text{m}^2$, which yields the periodicity $\Delta H = 0.2$ G according to the relation

$$\Delta HS = \Phi_0 \quad (23)$$

at various microwave power P levels, which is equivalent to certain values of the microwave-field amplitude and in the case shown in Fig. 3 of Ref. 8 we can put

$$H_1 / \Delta H = 2.4P^{1/2} / (\text{mW})^{1/2} .$$

There is a power threshold below which no MMMA signal is observed and the linewidth δH [field separation between the upper and the lower lobes of a line (see Fig. 2)] increases with increasing microwave-field amplitude.

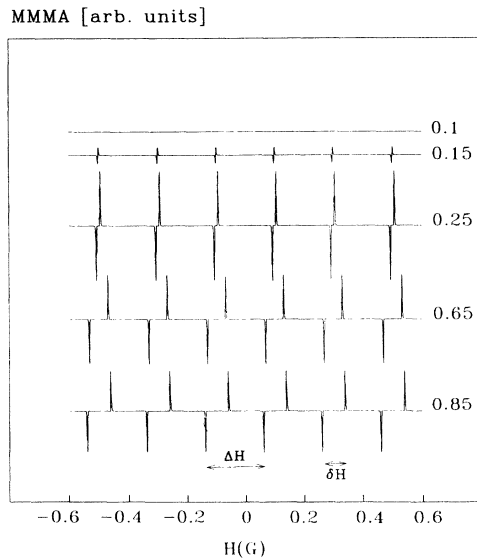


FIG. 2. The simulation of the dc scan MMMA spectra at various microwave power levels (in mW) as indicated. For $I_c = 3 \times 10^{-5}$ A, $\beta = 2.6$ at $T = 10$ K. ΔH is the periodicity of magnetic field and δH is the field separation between the upper and lower lobes of the line.

The intensity of the simulated signal slowly increases with increasing power, just as has been reported in experiment.⁸

TEMPERATURE DEPENDENCES

To determine the temperature dependence of MMMA signals one should first take into account temperature dependences of the parameters characterizing the rf SQUID. For single crystals of high-temperature superconductors with twin boundaries, it was shown^{8,9} that the cross-section area intercepting the magnetic flux detected by MMMA depends on temperature as

$$S(T) = S(0)(1-t^4)^{-1/2}, \quad \text{where } t = T/T_c. \quad (24)$$

It is explained by the fact that one of the dimensions of this area is determined by the penetration depth and the function from (24) is consistent with the empirical two-fluid model temperature dependence of the penetration depth. This effect becomes important only in temperatures close to the critical one. The value of the critical current is also a function of temperature, which can be taken into consideration assuming the BCS temperature dependence for the dielectric barrier Josephson junction¹⁵ approximated for our calculations by

$$I_c(T)/I_c(0) = (1-t^2). \quad (25)$$

Figure 3 presents the simulation of the MMMA signal at various temperatures for the same parameters as in Fig. 2. The result is in good agreement with the experimental data reported in Ref. 8.

Figure 4 shows plots of $\delta H / \Delta H$ versus $H_1 / \Delta H$ for several temperatures as indicated. Each plot gives a straight line described by

$$\delta H = 2(H_1 - H_{th}), \quad (26)$$

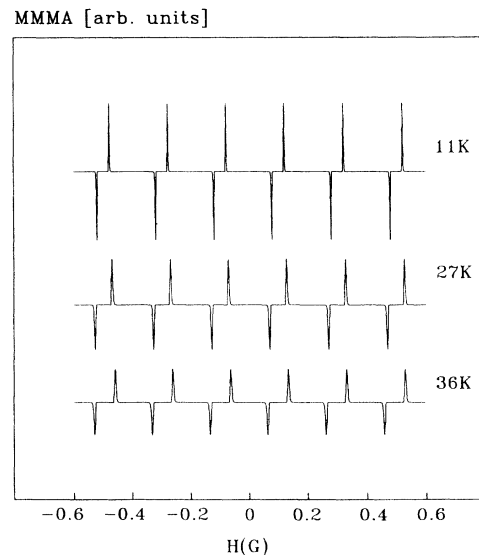


FIG. 3. Plots of dc scan spectra of MMMA simulation at various temperatures as indicated at a fixed microwave power level of 0.25 mW. I_c and β as in Fig. 2.

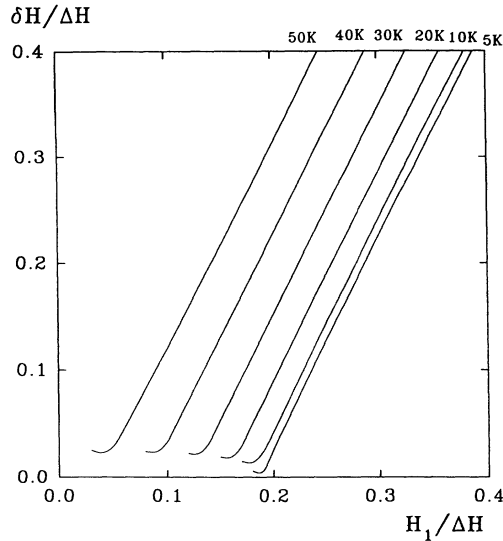


FIG. 4. The normalized linewidth $\delta H/\Delta H$ as a function of the microwave-field amplitude proportional to the square root of the incident microwave power, at various temperatures as indicated. I_c and β as in Fig. 2.

where H_{th} is the threshold value of H_1 . Relation (26) corresponds to the experimental data under the assumption that $H_1 \sim P^{1/2}$. The existence of a microwave power threshold is a consequence of the fact that if the amplitude of the variable magnetic field H_1 is too small to sweep the hysteresis loop, no MMMA signal can be observed and only after the H_1 amplitude has been increased above a threshold value H_{th} , can the system span the hysteresis loop. Figure 4 reveals for high temperatures certain characteristic curves in the dependence $\delta H(H_1)$ near the threshold value. At these temperatures δH does not reach zero although with decreasing H_1 the MMMA signal disappears. This phenomenon has been well visible in the experiment of Poppl *et al.*⁹ performed at a relatively high temperature of 77 K. In low temperatures this effect is much weaker.

The temperature dependence of δH is presented in Fig. 5 for several values of amplitudes H_1 of the microwave field. The width δH of the line increases with increasing temperature, which is attributed to two processes: the decreasing value of the power threshold which is strongly dependent on the critical-current value and increasing thermal fluctuations leading to an earlier jump over the higher potential barrier and decreasing the effective hysteresis loop. Figure 6 presents the signal intensity as a function of temperature for various amplitudes of H_1 . The MMMA signals for the parameters as in Fig. 2 disappear at a temperature T_0 of about 60 K as a consequence of the fact that the effective hysteresis and the power threshold tend to zero at this temperature. In such circumstances, the system under the influence of significant fluctuations does not differentiate shallow metastable states and begins working in the dispersive mode.

We have also investigated the temperature dependence of the microwave power threshold. Figure 7 presents the

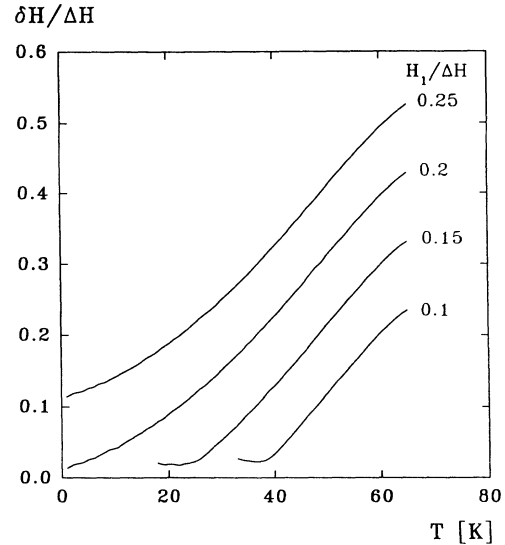


FIG. 5. Plots of the normalized linewidth $\delta H/\Delta H$ as a function of temperature for several values of the normalized microwave-field amplitude as indicated. I_c and β as in Fig. 2.

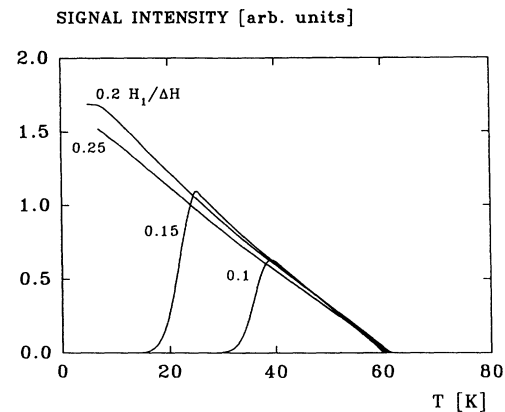


FIG. 6. Temperature dependence of the intensity of the MMMA signal for several values of the normalized microwave-field amplitude as indicated. I_c and β as in Fig. 2.

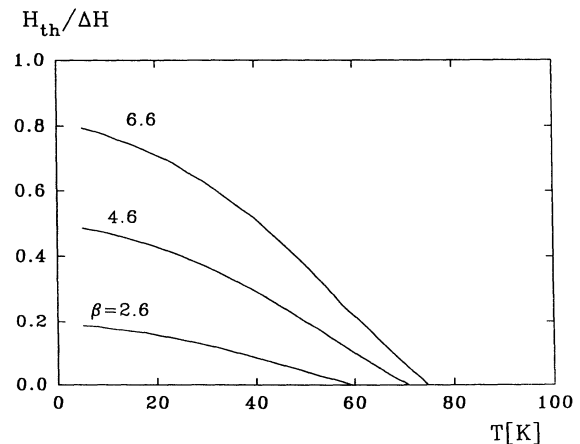


FIG. 7. Plots of microwave amplitude threshold as a function of temperature for several values of β as indicated. I_c as in Fig. 2.

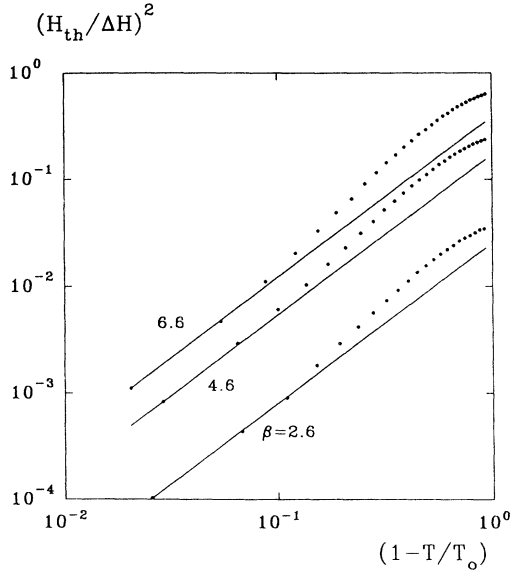


FIG. 8. Log-log plot of the square of the microwave-field threshold H_{th} as a function of $(1 - T/T_0)$, where T_0 is the temperature at which absorption disappears. These temperature dependencies are compatible with $(1 - T/T_0)^{3/2}$ as indicated by the solid lines.

plots of $H_{th}/\Delta H$, the amplitude of the microwave field for the threshold value as a function of temperature for several values of β as indicated and for $I_c = 3 \times 10^{-5}$ A. The value of H_{th} was determined from the intersection of the straight line [Eq. (26)] with the microwave amplitude axis (Fig. 4). The microwave power threshold disappears at the same temperature T_0 as the MMMA signal, which is much lower than critical temperature T_c of the superconducting state. When the parameter β increases, the value of the temperature T_0 also increases getting close

$$I_c(H)/I_c(0) = \begin{cases} |\sin(\pi\Phi_j/\Phi_0)/(\pi\Phi_j/\Phi_0)|, & \text{for } |\Phi_j| \leq \Phi_0/2 \\ |1/(\pi\Phi_j/\Phi_0)|, & \text{for } |\Phi_j| > \Phi_0/2. \end{cases} \quad (28)$$

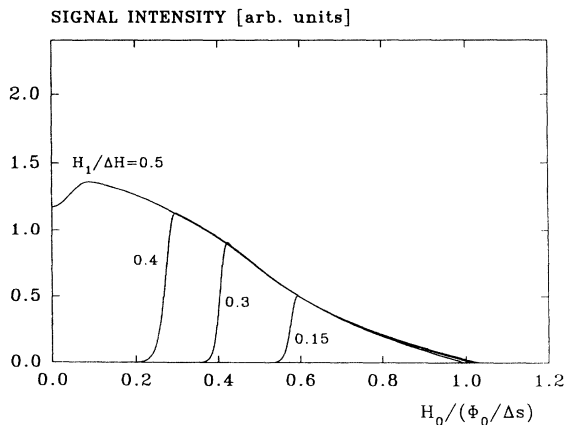


FIG. 9. Signal intensity as a function of the dc magnetic field for several values of the normalized microwave-field amplitude as indicated. Δs is the area of the Josephson junction. $T = 3$ K, $I_c = 1.5 \times 10^{-5}$ A, $\beta = 5.1$.

to T_c . To compare our numerical simulations with experimental data we present in Fig. 8 a log-log plot of $H_{th}^2/\Delta H^2$ as a function of normalized temperature $(1 - T/T_0)$. The $H_{th}^2/\Delta H^2$ approaches zero at T_0 compatible with a $(1 - T/T_0)^{3/2}$ law. The experimental results reported by Blazey, Portis, and Holtzberg¹⁰ have been described by this relation provided that $T_0 = T_c$, which is consistent with our model for high values of the parameters β and I_c . Moreover, the values of $H_{th}^2/\Delta H^2$ higher than implied by this relation for temperatures $(1 - T/T_0) > 0.1$ are also in agreement with the Blazey observations.¹⁰

MAGNETIC-FIELD EFFECT

A characteristic property of the periodic MMMA spectra in superconductors is the dependence of the MMMA lines intensity on dc magnetic field, which has been presented in many works.^{5,6,9} This dependence can be of different character. The signal disappeared for the fields of the intensities corresponding to from a few to few hundreds periods. In low temperatures, a new effect has been observed that is a threshold value of the dc magnetic field at which the periodic structure of MMMA spectra appears. This phenomenon can be explained taking into account that the magnetic flux threads the Josephson junction of a finite effective area Δs . In such conditions the value of the critical current of the junction satisfies the relation

$$I_c(H)/I_c(0) = \left| \frac{\sin(\pi\Phi_j/\Phi_0)}{\pi\Phi_j/\Phi_0} \right|, \quad (27)$$

where $\Phi_j = H\Delta s$ is the flux threading through the junction. In our calculations, we approximated Eq. (27) by the following:

Equation (28) describes the envelope of the function (27). Figure 9 presents numerical simulation of the MMMA signal intensity as a function of the dc field for several values of the microwave-field amplitude at 3 K for $J_c = 1.5 \times 10^{-5}$ A and $\beta = 5.1$. One can find considerable resemblance between our results and those of Dulcic, Crepeau, and Freed,⁶ who reported that at low power values, the MMMA lines appeared only for high magnetic field. The initial increase in the microwave power brings about a rapid increase in the intensity of the lines near the zero magnetic field, but with further increasing of the power, the MMMA signal amplitude is constant.

THE MICROWAVE SCAN

Kish, Tyagi, and Kraft⁸ have studied the MMMA signal as a function of the microwave field at nominally zero dc field (the microwave scan). When H_1 has been increased, the system would be taken through more than

one hysteresis loop. If the amplitude H_1 is large enough to take the system through several hysteresis loops then, as H_1 is swept, several transitions will occur (Fig. 10). The results of the experiment⁸ can be simulated using Eq. (25). However, for the zero magnetic field we will not get the MMMA spectrum, despite the fact that microwave absorption takes place there, because the MMMA signals of opposite phases overlap and do not produce a resultant signal. In Ref. 8 it was mentioned that the external magnetic field was not greater than 20 mG. Assuming $T=62$ K, $I_c=7.8 \times 10^{-5}$ A, $\beta=21$, and the nonzero value of dc field $H_0/\Delta H=0.13$ we obtained a band of lines very similar to the experimental one, but the signal amplitude was constant and did not decrease monotonously with the microwave-field amplitude. The authors of the experiment⁸ pointed out that the loop with a junction active in the microwave scan was different from the one that was observed in the dc scan experiment (Fig. 2). Their conclusion has been confirmed by the fact that we had to choose different parameters to describe these two cases, i.e., dc scan and the microwave scan. For the second case we found that ΔH was about 40 mG so for $H_0/\Delta H=0.13$, $H_0=5.2$ mG, which is within the limits of the residual 20 mG. Also, the effective junction area Δs was different in the cases of microwave and dc field scan. In order to reproduce the effect of the signal's amplitude decrease, we have analyzed the effect of the microwave field penetrating into the junction on the value of its critical current¹⁵ using Eq. (28). Figure 10 presents the numerical simulation of the microwave scan experiment obtained under the assumption that the effective junction area is $\Delta s=0.15S$. The absence of MMMA signal for the nominally zero value of dc field explains the observations reported in Ref. 8, i.e., that only a single loop with a junction was activated during the microwave scan, while a series of them were activated during the dc field scan, that is, only for this one loop the $H_0/\Delta H$ ratio was sufficiently high.

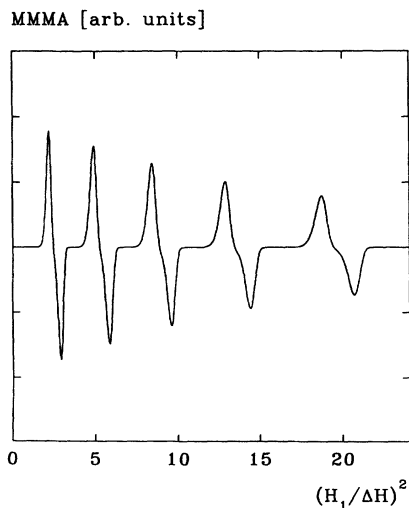


FIG. 10. Plots of the simulation of the MMMA as a function of the square of the incident microwave-field amplitude (the microwave scan) at $T=62$ K, $I_c=7.8 \times 10^{-5}$ A, $\beta=21$.

DISCUSSION

We agree with the conception that the origin of the superconducting current loops is related to the planar defects appearing in the form of twin boundaries in single crystals of cuprate superconductors.⁷ Because of a very short coherence length of this material, these planar defects act as Josephson junctions. We suggest, that the magnetic field enters homogeneously the twin boundaries so that the current crosses the plane of the defect only close to the edge, forming a quasi-one-dimensional superconducting loop with two junctions at the edges. This idea has been confirmed by the experiment in which the periodicity of the MMMA signal was observed to increase twice as a result of having divided an Y-Ba-Cu-O monocrystal into two equal parts along the plane perpendicular to the plane of the twinning.

The proposed phenomenological model of the microwave absorption of a superconducting ring connected by the Josephson junction has been adequately compared to the available experimental data of periodic microwave absorption in single crystals of cuprate superconductors and for special cases of low-temperature superconductors. The model has been developed on the basis of a number of simplifying assumptions, which means that it is fully correct only within certain limits. At sufficiently high frequencies, the response of the SQUID to the applied flux is effected by the L/R time constant of the SQUID. In general, for $\omega \ll R/L$, φ_x changes sufficiently slowly that φ always manages to settle in a local minimum of energy U and when the barrier ΔU separating a local minimum from the next lower minimum disappears, φ makes an abrupt transition to the lower minimum. When $\omega > R/L$, φ is driven through the potential-energy valley so quickly that it cannot settle at the bottom of the local minima. Although φ_x is much higher than the value at which the barrier to the next minimum disappears, our system does not undergo a transition. For Y-Ba-Cu-O the time L/R is about 10^{-12} s so the condition $\omega=9.4$ GHz $\ll R/L$ is valid, but for traditional superconductors this time can be lower.²⁰⁻²² However, in this work it is assumed that the SQUID behaves similarly as it is expected to behave at lower frequencies. For a high-frequency limit the microwave absorption is still possible, but the model of this phenomenon should be based on the extended version of Eq. (1), assuming a sinusoidal current-phase relation and negligible capacitance;²³

$$\varphi + \beta \sin(\varphi) + L \frac{d\varphi}{dt} / R = \varphi_x. \quad (29)$$

Buhrman and Jackel²³ have analyzed the behavior of the rf SQUID using (29) for a high-frequency limit and they found that the intrinsic noise amplitude closely approaches the classical limit for $\omega > R/L$.

Our model of MMMA works provided that the condition (19) is satisfied. If it is not, the aperiodic character of absorption, leading to the fluctuations of the ac field amplitude, becomes important and may bring about an increase in the width of the lobes of the MMMA lines.

The temperature dependence of the Josephson junction critical current has been approximated by (25), which can be expressed in a different form for a specific junction depending on its type and shape. Equation (24) will not be important for systems in which the loop surface is not quasi-one-dimensional. We have also assumed that the frequency ω_c and inductance L of the loop are independent of temperature, which is a good approximation for most cases.

From (4), one can estimate the value of the energy dissipated by the system in traversing a single hysteresis loop. For the parameters used in simulations, the absorbed power is of an order of 1 nW. This energy is dissipated as heat or to a lesser degree radiated as electromagnetic waves but finally most of it is thermalized. In the microwave scan experiment, when the amplitude of the microwave field is increased, in a single cycle we traverse an increasing number of hysteresis loops which multiplies the absorbed power. Then, the power absorbed by the SQUID may significantly increase the temperature of the system, inducing changes in its parameters. In the case of the microwave scan, this would lead to a decrease in the MMMA signal amplitude for high microwave power, however, it is difficult to estimate this process quantitatively.

It was found that high-temperature superconductors in forms of ceramics, powders, and single crystals generate higher-harmonic components of magnetization when immersed in an ac magnetic field. To explain these phenomenon various theoretical descriptions have been proposed, such as the model of loops with weak links^{13,24} and the macroscopic critical-state model.²⁵ In our opinion, these two alternative models do not exclude each other and both proposed processes can occur simultaneously. For example, in twinned monocrystalline samples, due to their high critical currents, a significant contribution may come from the network of inductive loops with Josephson junctions. In the studied model of the rf SQUID, the generation of harmonics will also take place. We can give an approximate analytical equation describing this process, using our model. The magnetic moment m of the loop for flux $\varphi_x(t) = \hat{\varphi}_x + a \sin(\omega t)$ is

$$m(t) \sim SI = m_0 i = \frac{m_0}{\beta} [\varphi_x - \varphi]. \quad (30)$$

For $|\hat{\varphi}_x| < \pi/2$ and $\varphi_{th} + \frac{5}{2}\pi > a > \varphi_{th} + \frac{3}{2}\pi$, the internal flux φ can be approximated by using the step function $\Theta(x)$:

$$\varphi = 2\pi [\Theta(t - t_1) - \Theta(t - t_2) - \Theta(t - t_3) + \Theta(t - t_4)], \quad (31)$$

where t_1, t_2, t_3 , and t_4 satisfy the following relations:

$$\begin{aligned} a \sin(\omega t_1) &= \pi + \varphi_{th} - \hat{\varphi}_x, \\ a \sin(\omega t_2) &= \pi - \varphi_{th} - \hat{\varphi}_x, \\ a \sin(\omega t_3) &= -\pi - \varphi_{th} - \hat{\varphi}_x, \\ a \sin(\omega t_4) &= -\pi + \varphi_{th} - \hat{\varphi}_x. \end{aligned} \quad (32)$$

Expanding $m(t)$ in a Fourier series one gets

$$m(t) = \frac{m_0}{\beta} \left[a_0 + \sum_{n=1}^{\infty} [a_n \cos(n\omega t) + b_n \sin(n\omega t)] \right], \quad (33)$$

where a_0 is the dc component and

$$\begin{aligned} a_n &= \frac{2}{n} [-\sin(n\omega t_1) + \sin(n\omega t_2) \\ &\quad + \sin(n\omega t_3) - \sin(n\omega t_4)], \\ b_n &= -\frac{2}{n} [\cos(n\omega t_1) - \cos(n\omega t_2) - \cos(n\omega t_3) \\ &\quad + \cos(n\omega t_4) - a \delta_{n1}/2]. \end{aligned} \quad (34)$$

For a special case of zero dc field, we obtain $\omega t_3 = \pi + \omega t_1$ and $\omega t_4 = \pi + \omega t_2$, and the magnetic moment is then nonzero only for the odd harmonics, which is in agreement with experimental data.^{24,25} The power in the n th harmonic is related to $P(n\omega) \sim (m_0/\beta)^2 (a_n^2 + b_n^2)$, which for zero dc field gives the envelope of the spectrum of the odd harmonics $1/n^2$ in consistence with experimental results.^{24,25} Thus, the model we have assumed also explains generation of harmonic components of electromagnetic response in the studied superconducting samples.

CONCLUSION

The model of the rf SQUID with thermal fluctuations has been used to explain the phenomenon of the periodic MMMA in single crystals of cuprate superconductors and low-temperature superconductors. Analytical expressions describing the shape of a single of MMMA spectra are given. A good agreement between the model predictions and the earlier experimental data on the temperature, magnetic-field, and microwave dependences of MMMA has been obtained. The mechanism of disappearance of the periodic absorption for temperatures lower than the critical one has been explained. The proposed model also permitted simulating the spectrum obtained from the microwave scan. Investigation of the MMMA signal of granulated samples would require a consideration of a network of Josephson junctions and inductive loops of various areas and orientations taking into account the interaction between the loops via mutual inductance.

ACKNOWLEDGMENTS

This work was supported in part by KBN Grant No. 2 0976 91 01.

- ¹R. Durny, J. Hautela, S. Ducharme, B. Lee, O. G. Symko, P. C. Taylor, D. Z. Zheng, and J. A. Xu, *Phys. Rev. B* **36**, 2361 (1987).
- ²J. Stankowski, P. K. Kahol, N. S. Dalal, and J. S. Moodera, *Phys. Rev. B* **36**, 7126 (1987).
- ³K. W. Blazey, K. A. Muller, J. G. Bednorz, W. Berlinger, G. Amoretti, E. Buluggiu, A. Vera, and F. C. Maticotta, *Phys. Rev. B* **36**, 7241 (1987).
- ⁴J. Stankowski and B. Czyzak, *Appl. Magn. Res.* **2**, 465 (1991).
- ⁵K. W. Blazey, A. M. Portis, K. A. Muller, and F. H. Holtzberg, *Europhys. Lett.* **4**, 457 (1988).
- ⁶A. Dulcic, R. H. Crepeau, and J. H. Freed, *Physica C* **160**, 223 (1989).
- ⁷H. Vichery, F. Beuneu, and P. Lejay, *Physica C* **159**, 823 (1989).
- ⁸K. Kish, S. Tyagi, and C. Kraft, *Phys. Rev. B* **44**, 225 (1991).
- ⁹A. Poppl, K. Kevan, H. Kimura, and R. N. Schwartz, *Phys. Rev. B* **46**, 8559 (1992).
- ¹⁰K. W. Blazey, A. M. Portis, and F. H. Holtzberg, *Physica C* **157**, 16 (1989).
- ¹¹J. E. Drumheller, Z. Trybula, and J. Stankowski, *Phys. Rev. B* **41**, 4743 (1990).
- ¹²A. S. Kheifets and A. I. Veinger, *Physica C* **165**, 491 (1990).
- ¹³T. K. Xia and D. Stroud, *Phys. Rev. B* **39**, 4792 (1989).
- ¹⁴A. H. Silver and J. E. Zimmerman, *Phys. Rev.* **157**, 317 (1967).
- ¹⁵See, A. Barone and G. Paterno, *Physics and Application of the Josephson Effect* (Wiley, New York, 1982).
- ¹⁶K. K. Likhariiev and B. T. Ulrich, *Josephson Junction Circuits and Applications* (Izd. Mosk. Universiteta, Moscow, 1978).
- ¹⁷J. Kurkijarvi, *Phys. Rev. B* **6**, 832 (1972).
- ¹⁸J. Kurkijarvi and W. W. Webb, *Proceedings of the Applied Superconductivity Conference*, Annapolis, IEEE Pub. No. 72CMO682-57ABSC (IEEE, New York, 1972), p. 581.
- ¹⁹V. I. Muromtsev, V. V. Troitskii, I. O. Maslennikov, M. A. Krykin, and A. A. Bush, *Physica C* **194**, 71 (1992).
- ²⁰K. P. Daly, I. Burch, S. Coons, and R. Hu, *IEEE Trans Magn. MAG-27*, 3066 (1991).
- ²¹E. M. Gershonzon, G. N. Goltsman, A. L. Dzordanov, and M. A. Zorin, *IEEE Trans. Magn. MAG-27*, 2844 (1991).
- ²²M. Muck, *IEEE Trans. Appl. Supercond.* (to be published).
- ²³R. A. Buhrman and L. D. Jackel, *IEEE Trans. Magn. MAG-13*, 879 (1977).
- ²⁴C. D. Jeffries, Q. H. Lam, Y. Kim, C. M. Kim, and A. Zettl, *Phys. Rev. B* **39**, 11 526 (1989).
- ²⁵L. Ji, R. H. Sohn, G. C. Spalding, C. J. Lobb, and M. Tinkham, *Phys. Rev. B* **40**, 10936 (1989).